

- 1 **Running Head:** CCM regulation in synchronised *Chlamydomonas*
- 2 **Corresponding Author:** Howard Griffiths
- 3 **Address:**
- 4 Department of Plant Sciences
- 5 University of Cambridge
- 6 Downing Street
- 7 Cambridge CB2 3EA
- 8 United Kingdom
- 9 **Telephone:** +44 1223 333 900
- 10 **Email:** hg230@cam.ac.uk
- 11 **Research area:** Biochemistry and Metabolism

12 **Title of Article:**

13 **Dynamics of carbon concentrating mechanism induction and protein re-localisation**
14 **during the dark to light transition in synchronised *Chlamydomonas***

15 Madeline C. Mitchell¹, Moritz T. Meyer¹ and Howard Griffiths^{1*}

16 ¹Department of Plant Sciences, University of Cambridge, Downing Street, Cambridge CB2
17 3EA, United Kingdom

18 **One sentence summary:** In synchronised *Chlamydomonas reinhardtii* cells, the carbon
19 concentrating mechanism is induced prior to dawn, which coincides with the re-localisation
20 of key proteins to the chloroplast pyrenoid.

21 **Footnotes:** M.C.M. is a Herchel Smith Research Student (University of Cambridge). This
22 research was supported by Biotechnology and Biological Sciences Research Council Grant
23 BB/I024518/1 (“Combining Algal and Plant Photosynthesis”).

24 ***Corresponding Author:** Howard Griffiths

25 **Abstract**

26 In the model green alga *Chlamydomonas reinhardtii*, a carbon concentrating mechanism
27 (CCM) is induced under low CO₂ in the light and comprises: active inorganic carbon
28 transport components, carbonic anhydrases and aggregation of Rubisco in the chloroplast
29 pyrenoid. Previous studies have focused predominantly on asynchronous cultures of cells
30 grown under low versus high CO₂. Here, we have investigated the dynamics of CCM
31 activation in synchronised cells grown in dark/light cycles, as compared to induction under
32 low CO₂. The specific focus was to undertake detailed time course experiments comparing
33 physiology and gene expression during the dark to light transition. Firstly, the CCM could be
34 fully induced one hour before dawn, as measured by the K_{0.5} for inorganic carbon (C_i). This
35 occurred in advance of maximum gene transcription and protein accumulation and
36 contrasted with the co-ordinated induction observed under low CO₂. Between two hours and
37 one hour before dawn, the proportion of Rubisco and the thylakoid lumen carbonic
38 anhydrase, CAH3, in the pyrenoid rose substantially, coincident with increased CCM activity.
39 Thus, other mechanisms are likely to activate the CCM before dawn, independent of gene
40 transcription of known CCM components. Furthermore, this study highlights the value of
41 using synchronised cells during the dark to light transition as an alternative means of
42 investigating CCM induction.

43 INTRODUCTION

44 Carbon concentrating mechanisms (CCMs) have evolved in most unicellular aquatic
45 photosynthetic organisms to compensate for the kinetic constraints of the primary
46 carboxylase Rubisco (Spreitzer and Salvucci, 2002) and limited availability of $\text{CO}_{2(\text{aq})}$. In
47 eukaryotic algae (Giordano et al., 2005, Moroney and Ynalvez, 2007, Wang et al., 2011) and
48 cyanobacteria (Price et al., 2008), these CCMs are biophysical means of concentrating CO_2
49 around Rubisco, thereby favouring the carboxylation reaction and improving growth in CO_2 -
50 limited environments.

51 In the model green alga *Chlamydomonas reinhardtii*, three elements are important for CCM
52 activity: first, inorganic carbon (Ci) transporters at the plasma membrane and chloroplast
53 envelope (Spalding, 2008); second, carbonic anhydrases which facilitate the interconversion
54 of CO_2 and HCO_3^- and operate in parallel within each cellular compartment (Moroney et al.,
55 2011); and third, the localisation of Rubisco to a chloroplast microcompartment called the
56 pyrenoid to minimise CO_2 leakage (Ma et al., 2011, Meyer et al., 2012). The CCM is induced
57 at low (air level) CO_2 concentrations, resulting in an increased whole cell affinity for Ci and
58 internal Ci accumulation (Badger et al., 1980), coincident with the *de novo* synthesis of
59 several proteins (Manuel and Moroney, 1988).

60 Further candidate CCM genes have been identified as low CO_2 -induced through microarray
61 and transcriptomic studies (Miura et al., 2004, Yamano et al., 2008, Brueggeman et al.,
62 2012, Fang et al., 2012) or by isolating mutants with reduced growth or Ci accumulation at
63 low CO_2 (for example, Spalding et al., 1983; Colombo et al., 2002; Thyssen et al., 2003).
64 Low CO_2 -induced genes investigated in this study include several Ci transporter candidates,
65 some of which are amongst the most highly induced genes under low CO_2 (Brueggeman et
66 al., 2012). *HLA3* encodes a plasma membrane-localised ABC-type transporter (Duanmu et
67 al., 2009), *LCI1* encodes another plasma membrane transporter (Ohnishi et al., 2010), and
68 *LCIA*, *CCP1* and *CCP2* all encode proteins putatively involved in Ci transport and associated
69 with the chloroplast envelope (Wang et al., 2011).

70 Two carbonic anhydrases were also of interest. The *CAH1* gene encodes a periplasmic
71 carbonic anhydrase and is highly CO_2 -responsive, although *CAH1*-deficient mutants retain a
72 functional CCM (Van and Spalding, 1999). *CAH3* encodes a thylakoid-luminal carbonic
73 anhydrase essential for growth at ambient CO_2 , although the gene is minimally CO_2 -
74 responsive and the protein is expressed equally under high and low CO_2 (Karlsson et al.,
75 1998).

76 Expression of other CCM-related genes was also determined, including *LCR1*, which
77 encodes a MYB-domain transcription factor upstream of *CAH1* and *LCI1* and downstream of
78 CCM master regulator CIA5 (Yoshioka et al., 2004). LCIB and LCIC, which form a peri-
79 pyrenoidal complex associated with carbon recapture (Wang and Spalding, 2013), were also
80 included in this study, as were *RBCS* and *rbcL*, which encode the small and large subunits
81 of Rubisco, the major pyrenoid component (Borkhsenius et al., 1998).

82 In addition to CO₂ responsiveness, CCM activity in *Chlamydomonas* is associated with light
83 and photosynthesis. In particular, accumulation of Ci in *Chlamydomonas* cells and
84 chloroplasts is light-dependent (Spalding and Ogren, 1982) and may be driven by ATP from
85 cyclic electron transport (Spalding et al., 1984). HLA3 is a member of the ATP-binding
86 cassette superfamily, which suggests light-dependency, and *HLA3* expression is inhibited by
87 DCMU and in photosystem I and photosystem II mutants (Im and Grossman, 2002).
88 Although originally identified as a high light-induced gene, *HLA3* may in fact be responding
89 to low CO₂ levels brought about by increased photosynthesis at higher light intensities,
90 consistent with the induction of other CCM genes under these conditions (Im and Grossman,
91 2002). Similarly, *CAH1* transcription requires light, low CO₂ and photosynthetic electron flow
92 (Dionisio-Sese et al., 1990). At the protein level, the LCIB-LCIC complex relocates from the
93 stroma to the area around the pyrenoid both in response to light and to CO₂ levels (Yamano
94 et al., 2010). However, cells acclimating to low CO₂ induce external CA activity and active
95 HCO₃⁻ transport even in the dark, although induction is delayed compared to cells switched
96 to low CO₂ in the light (Bozzo and Colman, 2000). This suggests that light, while an
97 important regulator of CCM activity, is not an absolute requirement for expression of CCM
98 components. Indeed, in synchronised cells grown at ambient CO₂, genes encoding putative
99 Ci transporters and mitochondrial carbonic anhydrases are transcriptionally upregulated in
100 the light, whereas other key CCM gene transcripts (*CAH3*, stromal carbonic anhydrase
101 *CAH6*, *LCIB*) reach maximum levels during the last half of the dark period (Tirumani et al.,
102 2014).

103 While the majority of experiments investigating CCM induction have used cells in
104 asynchronous cultures grown in continuous light, the aim of the present study was to
105 investigate the dynamics of CCM induction and molecular regulation in synchronised cells
106 grown in dark/light cycles, focussing on a detailed time course during the dark to light period
107 transition. Given the apparent down-regulation of the CCM in the dark (Marcus et al., 1986),
108 we hypothesised that induction of the CCM during the dark to light transition might involve
109 non-transcriptional/translational mechanisms regulating existing CCM components, unlike
110 the CO₂ response, which requires strong transcriptional up-regulation and *de novo* protein
111 synthesis.

112 To investigate possible mechanisms of CCM regulation in synchronised cells, whole cell
113 affinity for Ci ($K_{0.5}$) as well as the relative abundance of known CCM (CO_2 -responsive) gene
114 transcripts and proteins were measured across the dark to light transition and
115 unsynchronised cultures adapting to low CO_2 were used as a control. We also set out to
116 determine the extent that the thylakoid luminal CAH3 and Rubisco relocalised from the
117 stroma to the pyrenoid during the dark to light transition, since this preferential localisation
118 appears to be required for a fully functioning CCM (Blanco-Rivero et al., 2012, Meyer et al.,
119 2012).

120 Unsynchronised cells adapting to low CO_2 showed rapid increases in mRNA levels of CCM
121 genes, followed by increased protein abundance and then CCM activity. In synchronised
122 cells, CCM activity was initially down-regulated in the dark but full CCM activity was inducible
123 before dawn and also prior to maximum mRNA and protein accumulation. Rubisco and
124 CAH3 were both found to have re-localised to the pyrenoid, coincident with increased CCM
125 activity.

126 **RESULTS**

127 **The CCM is partially repressed in the dark but can be induced one hour before dawn**

128 CCM induction during the dark to light transition was measured at the whole cell and
129 molecular level to identify factors affecting CCM regulation in synchronised cultures. Whole
130 cell affinity for Ci ($K_{0.5}$) was derived using an oxygen electrode and HCO_3^- -addition
131 responses, following a light pre-treatment used to deplete residual inorganic carbon
132 supplies. In synchronised cells, $K_{0.5}$ for Ci was measured from two hours before dawn to six
133 hours after dawn (Fig. 1A). A relatively high $K_{0.5}$ value ($60 \mu\text{M Ci}$) was found towards the end
134 of the dark period (-2 h), indicating that the CCM was at least partially repressed in the dark,
135 even after the short light pre-treatment. From this time point, CCM inducibility rapidly
136 increased, so that one hour before dawn, cells were able to express a fully functioning CCM
137 (as indicated by a low $K_{0.5}$ of $11 \mu\text{M Ci}$). This high affinity for Ci was maintained through
138 dawn and the first six hours of the light period (mean $K_{0.5}$ of 11 to $19 \mu\text{M Ci}$).

139 In order to provide a direct comparison for dark-to-light time courses, CCM induction in
140 asynchronous cultures grown in continuous light and switched to low CO_2 was also
141 investigated. The very high $K_{0.5}$ value ($240 \mu\text{M Ci}$) of high CO_2 -adapted cells indicated that
142 the CCM was fully repressed at the beginning of the time course (Fig. 1B). Affinity for Ci
143 rapidly increased following the transfer to low CO_2 , with the measured $K_{0.5}$ reduced to 105
144 $\mu\text{M Ci}$ within one hour of the shift to low CO_2 . Cells showed maximum CCM induction
145 (highest affinity for Ci) after 4-6 h at low CO_2 , as indicated by low $K_{0.5}$ values ($25\text{-}40 \mu\text{M Ci}$).

146 The maximum $K_{0.5}$ value measured for high CO_2 -adapted cells was greater than that
147 observed in dark-adapted (-2 h) cells, as was the overall decrease in $K_{0.5}$ during each time
148 course (ten-fold and six-fold, respectively), which suggests that the CCM was repressed to a
149 greater extent at high CO_2 than two hours before dawn.

150 **Maximum gene expression occurs after CCM induction during the dark to light**
151 **transition**

152 In this comparative study between CCM regulation during the dark to light transition and the
153 conventional CO_2 response, qRT-PCR was used to track expression of CO_2 -responsive
154 genes. Gene expression was quantified relative to the control gene *GBLP* and to the first
155 time point. In synchronised cells two hours before dawn, *CCP1*, *CCP2*, *LCI1*, *LCIA*, *LCIB*
156 and *LCIC* were all present at similar levels to high CO_2 -adapted cells (Supplemental Table
157 S1). *CAH1*, *LCR1* and *rbcL* were present in greater abundance while *HLA3* and *RBCS* were
158 present in lesser abundance in dark/light-grown (-2D) compared to high CO_2 -grown (0 h)
159 cells. Maximum levels of *CAH1*, *CCP1*, *LCI1*, *LCIA*, *LCIB* and *LCIC* mRNA were not
160 significantly different between dark/light and CO_2 time courses (Supplemental Table S2).
161 Some differences were observed in the maximum abundance of *CCP2*, *HLA3*, *LCR1*, *rbcL*
162 and *RBCS* but these were below one order of magnitude and smaller than the differences
163 observed at the beginning of the time courses. Overall, this indicates that transcriptional
164 regulation during CCM induction in response to light is similar to that of CO_2 .

165 Indeed, in synchronised cells, many CO_2 -responsive genes (*CCP1*, *CCP2*, *LCI1*, *LCIA*, *LCIB*
166 and *LCIC*) were upregulated during the light period to a similar extent as for the CO_2
167 response (Fig. 2, Supplemental Tables S3 and S4). However, the majority of transcriptional
168 upregulation did not occur until several hours after maximum CCM activity was observed
169 (Fig. 1A, Fig. 2; see also Supplemental Fig. S1 and Table S2), contrasting with the
170 concurrent CCM activation and low CO_2 -induced gene induction observed in cells adapting
171 to low CO_2 (Fig. 1B, Fig. 3; see also Supplemental Fig. S1 and Table S2).

172 Although CO_2 -responsive genes were consistently upregulated in the light, there were
173 systematic differences in the timing of maximum mRNA expression compared to the CO_2
174 response. For example, inorganic carbon transporter transcripts (*CCP1*, *CCP2*, *HLA3*, *LCI1*,
175 *LCIA*), *LCR1* and *CAH1* reached maximum levels between two and four hours after dawn,
176 whereas *LCIB* and *LCIC* levels were maximal just one hour into the light period (Fig. 2,
177 Supplemental Table S2). In contrast, CCM induction following transfer from high to low CO_2
178 showed a more co-ordinated response. CO_2 -responsive transcripts accumulated rapidly,
179 reaching maximum levels after approximately two hours and then showing a steady decline
180 over the next four hours (Fig. 3, Supplemental Table S2).

181 Additionally, because $K_{0.5}$ measurements required an initial period of pre-acclimation in the
182 light, gene expression was also measured in synchronised cells harvested before dawn after
183 a brief period of illumination in the oxygen electrode chamber (Fig. 2: -2L and -1L). This light
184 pre-treatment resulted in the strong upregulation of the Ci transporter genes *CCP1*, *CCP2*
185 *HLA3*, *LCI1* and *LCIA* but did not affect the expression of *CAH1* and *LCR1*. *LCIB* and *LCIC*,
186 although having a lower level of induction to begin with, also responded to the pre-dawn light
187 exposure.

188 *RBCS* (both *RBCS1* and *RBCS2*) mRNA levels remained largely unchanged throughout the
189 dark/light time course, including the pre-dawn light treatment (Fig. 2). *rbcL* transcripts
190 appeared to decrease in abundance by up to 80% both in response to the light treatment
191 and from dawn to six hours into the light, however overall abundance of both *RBCS* and *rbcL*
192 transcripts remained very high (at least one order of magnitude higher than the highly
193 abundant reference gene *GBLP*; Supplemental Tables S1 and S2). Similarly, only minimal
194 changes were detected in the abundance of genes encoding Rubisco (*RBCS* and *rbcL*)
195 throughout the CO₂ time course (Fig. 3).

196 **CCM repression in the dark is independent of key CCM protein abundance**

197 The abundance of several CCM proteins during the dark to light transition was measured
198 using immunoblots to determine whether increased mRNA abundance resulted in increased
199 protein levels (Fig. 4). To complement qRT-PCR data, pre-dawn samples (-2, -1) were
200 harvested either directly from the dark (D) or after light pre-treatment (L). Although CO₂-
201 responsive transcripts were present only at low levels two hours before dawn, their
202 corresponding proteins were easily detectable at this time. *LCIB* and *LCIC* were present at
203 high levels two hours before dawn, while CCM activity was still low. These proteins reached
204 maximum levels two to four hours into the light period, several hours after maximum CCM
205 activity occurred. *CAH1* was also detectable in the dark and did not show major changes in
206 abundance during the dark to light transition. No major change in either *RBCS* or *rbcL*
207 abundance was detected during this time course. Pre-dawn exposure to light (samples -2L
208 and -1L) had minimal effect on the abundance of all proteins probed.

209 In contrast, for cells adapting to low CO₂, immunoblot analyses of *LCIB*, *LCIC* and *CAH1*
210 showed co-ordinated increases in mRNA abundance and protein concentration (Fig. 5; see
211 also Supplemental Fig. S1). Unlike in dark-harvested (partially CCM-repressed)
212 synchronised cells, *LCIB*, *LCIC* and *CAH1* were almost undetectable in high CO₂-adapted
213 cells (Fig. 5: 0 h). However, all three proteins rapidly accumulated in response to low CO₂,
214 reaching maximum abundance after approximately three (*LCIB* and *LCIC*) to five hours

215 (CAH1) and maintaining these high levels for remainder of the time course. No changes in
216 rbcL or RBCS abundance were observed during the acclimation to low CO₂.

217 **Re-localisation of Rubisco and CAH3 to the pyrenoid coincides with CCM induction at** 218 **end of dark period**

219 Immunogold labelling was used to probe Rubisco and CAH3 localisation, which are both
220 known to be preferentially localised in the pyrenoid in response to low CO₂ (Fig. 6). Two
221 hours before dawn (-2D), approximately 75% of Rubisco-labelled particles were present in
222 the pyrenoid while, one hour later, almost 90% of labelled Rubisco was found in the pyrenoid
223 (-1D) and this high count was maintained two hours into the light period (2 h; Fig. 6A). This
224 change in Rubisco localisation coincided with the measured change in K_{0.5} but was
225 independent of the dark period light pre-treatment (-2L and -1L).

226 In contrast, relative CAH3 localisation changed both before dawn in the dark and in
227 response to pre-dawn light exposure (Fig. 6B). Two hours before dawn approximately 22%
228 of CAH3 particles were in the pyrenoid (-2D) but this proportion increased to 35% one hour
229 before dawn (-1D) and reached 40% two hours into the light period (2 h). The percentage of
230 CAH3 in the pyrenoid also responded directly to the pre-dawn light treatment (increasing to
231 33% at -2L and 39% at -1L).

232 In general, mean cell area increased in response to light exposure both before and after
233 dawn (Fig. 6C). Pyrenoid area also increased in line with cell area across the time course
234 (Fig. 6D).

235 **DISCUSSION**

236 Since Marcus et al. (1986) identified oscillations in both CCM activity and photosynthetic
237 characteristics in synchronised cells, the *Chlamydomonas* CCM has been characterised to a
238 much greater extent in asynchronous cells (see reviews: Moroney and Ynalvez, 2007, Wang
239 et al., 2011). The aim of this study was thus to reconcile changes at the molecular level with
240 regulation of overall CCM activity and cellular dynamics of key CCM constituents in a
241 detailed time course during the dark to light transition. Several key differences in CCM
242 induction were observed in synchronised, as compared to asynchronous cultures, as well as
243 the differential expression of known CCM genes in response to light. This study has
244 highlighted the possible importance of additional regulatory mechanisms since the CCM was
245 inducible before dawn, without concomitant increases in mRNA or protein levels of known
246 CCM components.

247 **Comparison of CCM induction in response to light and CO₂**

248 This study systematically characterised an eight hour period covering the dark to light
249 transition as well as the first six hours of acclimation to low CO₂ for comparison. Co-
250 ordinated increases in CCM mRNA and protein abundance support the idea that CCM
251 induction in response to low CO₂ relies on the *de novo* synthesis of many components. In
252 contrast, synchronised cells, which divide at the start of the dark period, can induce CCM
253 activity in advance of the light period and prior to increased expression of CCM gene
254 transcripts and proteins. Some CCM gene transcripts, mostly encoding Ci transporters, were
255 also found to respond differentially to pre-dawn light exposure.

256 The genes analysed by qRT-PCR in the current study (*CAH1*, *CCP1*, *CCP2*, *HLA3*, *LCI1*,
257 *LCIA*, *LCIB*, *LCIC*, *LCR1*) have all been assigned putative roles in the CCM and identified as
258 transcriptionally upregulated in response to low CO₂, in at least three of four microarray or
259 transcriptomic studies published to date (Brueggeman et al., 2012, Supplementary Dataset
260 1). Maximum abundance of these gene transcripts occurred after two hours at low CO₂ and
261 the average fold-change from high CO₂ levels was generally within five-fold of the values
262 obtained by Brueggeman et al., (2012) (see also Supplemental Table S4).

263 In synchronised cells, the level of gene induction (fold-increase) during the light period was
264 generally within one order of magnitude of that observed in cells adapting to low CO₂
265 (Supplemental Tables S3 and S4). Perhaps more importantly, the maximum levels of mRNA
266 abundance (relative to *GBLP*) were also within 4-fold of values obtained for the CO₂ time
267 course (Supplemental Table S2). Strong upregulation of CCM gene transcripts was thus
268 observed in synchronised cells but, crucially, this occurred only during the light period.
269 Maximum mRNA levels were reached approximately two hours into the light period when
270 cells had been expressing maximum CCM activity for the previous three hours.

271 Tirumani et al., (2014) also showed that Ci transporter transcripts were upregulated in the
272 light in synchronised cells of a different wild-type strain (137C/CC-125), which allows greater
273 confidence in the data given that differences between strains and growth conditions are
274 often a major source of variation between experiments (see for example, the discussion in
275 Brueggeman et al., 2012 and Fang et al., 2012). Tirumani et al., (2014) also showed that
276 gene expression for carbonic anhydrases (*CAH3*, *CAH6*) and *LCIB* was higher in the dark,
277 although this induction was suppressed by high CO₂. As with the different responses of CCM
278 genes to pre-dawn light treatment (discussed below), this suggests that CCM gene
279 transcription responds to multiple signals, and to light and low CO₂ in particular. In the
280 current study, expression of *LCIB* was measured from two hours before dawn, which may be
281 why this dark induction of key CCM genes was not observed. Expression of *CAH3* and

282 *CAH6* was not measured in this study because these genes are minimally responsive to
283 CO_2 . Finally, Tirumani et al., (2014) found that *CAH3* protein only accumulates during the
284 light period but, since they did not measure CCM activity or the abundance of *CAH6* and
285 *LCIB*, it is difficult to determine to what extent gene induction in the dark affects CCM
286 expression.

287 In the CO_2 response, *de novo* CCM protein expression was correlated with a large decrease
288 in $K_{0.5}$. qRT-PCR and immunoblot analyses for *LCIB* and *LCIC* showed maximum protein
289 abundance occurring approximately one hour after maximum mRNA abundance in both CO_2
290 and dark/light time courses. However, *LCIB* and *LCIC* were only slightly induced in the light
291 period compared to the large induction observed in response to low CO_2 . In contrast, *CAH1*
292 levels showed no increase during the light period despite increased transcription, which
293 again distinguishes this response from the large increases in transcription and translation
294 observed in response to low CO_2 . Overall, during the dark to light transition, minimal
295 induction of *CAH1*, *LCIB* and *LCIC* and the relatively high protein content in the dark were
296 consistent with both the lower $K_{0.5}$ and the inducibility of the CCM in the dark (Fig. 1A and 4).

297 **Transcriptional response to light pre-treatment and inducibility of the CCM in the dark**

298 Both the timing and speed of CCM induction in synchronised cells suggest that regulation
299 during the dark to light transition may not depend on the *de novo* synthesis of known CCM
300 proteins, in contrast to the low CO_2 response. The differential regulation of mRNA
301 expression and protein levels were further illustrated by the light pre-treatment used for
302 comparability with the protocol for $K_{0.5}$ measurements. Transcripts for inorganic carbon
303 transporters (*CCP1*, *CCP2*, *HLA3*, *LCI1*, *LCIA*) all responded strongly to the light pre-
304 treatment, generally reaching levels at least as high as those achieved one hour into the light
305 period of a conventional dark/light cycle. *LCIB* and *LCIC* transcripts, although induced to a
306 far lesser extent during the light period, showed a similar level of induction under pre-dawn
307 illumination. The speed and magnitude of this transcriptional response to light may be in part
308 due to the greater light levels in the oxygen electrode chamber (photon flux density 200-300
309 $\mu\text{mol photons m}^{-2} \text{ s}^{-1}$) compared to growth conditions in the incubator (50 $\mu\text{mol photons m}^{-2}$
310 s^{-1}). For example, mRNA levels of a CO_2 -responsive mitochondrial carbonic anhydrase
311 (*CAH4*) increase linearly with increasing light intensity up to 500 $\mu\text{mol photons m}^{-2} \text{ s}^{-1}$
312 (Eriksson et al., 1998), well above the intensities used in this study.

313 However, not all CCM-related gene transcripts showed the same pattern of induction in
314 response to pre-dawn light exposure. *LCR1*, although slightly induced during the light period,
315 did not respond to light before dawn. More notably, *CAH1* mRNA levels also did not change
316 in response to pre-dawn light exposure, despite being strongly upregulated during the

317 following light period. This indicates that *LCR1* and *CAH1* transcription may be regulated in a
318 different manner to other CO₂-responsive genes. Rawat and Moroney (1995) also identified
319 strong oscillations of *CAH1* transcripts in synchronised cells and *CAH1* was later shown to
320 be under circadian control (Fujiwara et al., 1996). The higher abundance of *CAH1* mRNA in
321 -2D (dark/light) cells compared to 0 h (CO₂) cells is consistent with the previous observation
322 of the presence of *CAH1* mRNA in cells at the end of the dark period (Supplemental Table
323 S1, Rawat and Moroney, 1995). This also explains the greater induction seen in the CO₂
324 response compared to dark/light-grown cells even though the maximum *CAH1* mRNA
325 abundance was similar in both time courses (Supplemental Table S2).

326 The evidence presented thus far suggests that the increased affinity for Ci ($K_{0.5}$) and
327 inducibility of the CCM in advance of the light period is uncoupled from the transcriptional
328 up-regulation of key CCM elements which occurred in the light, as distinct from low CO₂-
329 induced CCM activity. Secondly, the transcriptional responsiveness of inorganic carbon
330 transporter genes to pre-dawn light treatment, relative to other components, shows there to
331 be differentially regulated elements of the CCM. Together with the relatively high
332 concentrations of key CCM proteins in cells growing through dark and into light periods, this
333 leads us to suggest that post-translational mechanisms might be important for CCM
334 induction in synchronised cells during the dark to light transition.

335 **Dynamics of protein abundance and re-localisation during CCM induction across the** 336 **dark to light transition**

337 The relative localisation of mobile CCM components in synchronised cells was investigated
338 as a possible means of modulating CCM activity independently of protein abundance.
339 Importantly, Rubisco and CAH3 were found to be differentially localised during the dark to
340 light transition, although with certain key differences in this response.

341 Rubisco accumulated within the pyrenoid during the two hours before dawn, coinciding with
342 measured changes in $K_{0.5}$ values and suggesting that the aggregation of Rubisco in the
343 pyrenoid is associated directly with increased CCM activity. Brief exposure to light prior to
344 dawn did not affect Rubisco localisation, which suggests that changes in localisation during
345 the dark to light transition may rely on an endogenous (light-independent) signal.
346 Nevertheless, Rubisco is likely to respond to multiple signals because aggregation is also
347 known to occur in response to low CO₂ (Borkhsenius et al., 1998).

348 CAH3 localisation, like Rubisco, may also be controlled by an endogenous signal that co-
349 ordinates CCM induction. Two hours prior to dawn, 20% of CAH3 was localised to the
350 pyrenoid but one hour later the proportion of CAH3 in the pyrenoid had nearly doubled and

351 this high proportion was maintained two hours into the light period. However, in cells
352 harvested two hours before dawn and exposed briefly to light, the proportion of CAH3 in the
353 pyrenoid was also high. This suggests that CAH3 localisation could also be directly
354 regulated by light. This is consistent with qualitative data from immunofluorescence
355 experiments showing that, in synchronised cells CAH3 is distributed throughout the stromal
356 thylakoids in the middle of the dark period (-6 h) but is pyrenoid-localised in the middle of the
357 light period (6 h; Tirumani et al., 2014). However, the current quantitative study extends the
358 implications of these findings by showing relocalisation of CAH3 just prior to dawn (between
359 -2 and -1 h) in the dark and in response to pre-dawn illumination (at -2 h).

360 CAH3 re-localisation has also been observed in cells acclimating to low CO₂ and in the
361 current study CAH3 was present in the pyrenoid at similar relative abundance in dark-
362 versus light-adapted cells, compared to those adapted to high versus low CO₂ (19% and
363 37% respectively; Blanco-Rivero et al., 2012). In the CO₂ response, this shift in localisation
364 was linked to the phosphorylation of CAH3 (Blanco-Rivero et al., 2012) but it has not been
365 determined whether a similar mechanism is operating in air-grown synchronised cells. The
366 low CO₂-inducible protein, LCI5, is also rapidly phosphorylated in response to low CO₂ and
367 this has been shown to occur in a redox-dependent manner (Turkina et al., 2006). A similar
368 redox-dependent kinase may be responsible for phosphorylation of CAH3 in response to low
369 CO₂ and light; however, this would not explain the shift in CAH3 localisation in the dark.
370 Whatever the mechanism, the high relative localisation of CAH3 in the pyrenoid after the
371 light pre-treatment two hours before dawn may be partly responsible for the relatively low
372 K_{0.5} value (incomplete repression of the CCM) at this point.

373 **CONCLUSION**

374 Although there are similarities in the transcriptional response of genes during CCM induction
375 in response to low CO₂ and during the dark to light transition, this study has identified
376 several key differences that distinguish the response of synchronised cells from that of
377 asynchronous cultures. The inducibility of the CCM before dawn and in advance of mRNA
378 and protein accumulation was directly linked to increased localisation of Rubisco and CAH3
379 to the pyrenoid and highlights the potential importance of post-translational regulation of the
380 CCM. Further work will be needed to determine the mechanism of relocalisation of Rubisco
381 and CAH3 as well as to elucidate the pathways triggered in response to the different signals.
382 In any case, studies focussing on how components are modified, their subcellular
383 localisation and interactions will be necessary to further our understanding of the CCM.
384 Investigating these changes in synchronised cultures of cells during the dark to light

385 transition will provide additional means of probing these important aspects of CCM
386 regulation.

387 **MATERIALS AND METHODS**

388 **Algal strain and culture conditions:** The *Chlamydomonas reinhardtii* wild-type strain 2137
389 mt+ (Spreitzer and Mets, 1981) was maintained in the dark on Tris-acetate medium
390 (Spreitzer and Mets, 1981) agar plates supplemented with Kropat's trace elements (Kropat
391 et al., 2011). Liquid cultures were grown in an Innova 42 incubator (New Brunswick
392 Scientific, Enfield, CT, USA) at 25°C with 50 $\mu\text{mol photons m}^{-2} \text{ s}^{-1}$ illumination, aeration and
393 shaking (125 rpm). Starter cultures were inoculated into Tris-minimal (Tris-acetate without
394 acetate) medium from freshly replated Tris-acetate agar cells and grown to mid-log phase
395 ($1\text{-}2 \times 10^6$ cells mL^{-1}). Experimental cultures were inoculated from starter cultures and
396 harvested at mid-log phase. High CO_2 cultures were bubbled with 5% CO_2 for six days (one
397 starter followed by one experimental culture) before switching to bubbling with air (low CO_2 ;
398 0.04%) for the CO_2 response time course. Synchronised cultures were continuously bubbled
399 with air, grown in 12 h:12 h dark/light cycles and harvested when at mid-log phase during the
400 third light period after inoculation. Synchronicity of cell division under these conditions was
401 confirmed by cell counts over a 72 h period from inoculation to mid-log phase (harvest).

402 **Oxygen evolution measurements:** Apparent affinity for C_i was determined using the
403 oxygen evolution method described by Badger et al. (1980). Cells grown in Tris-minimal
404 liquid medium were harvested and resuspended in 25 mM HEPES-KOH (pH 7.3) to a
405 density of 1.5×10^7 cells mL^{-1} . Aliquots of cells (1 mL) were added to a Clark type oxygen
406 electrode chamber (Rank Brothers, Cambridge, UK) attached to a circulating water bath set
407 to 25 °C. The chamber was closed for a light pre-treatment (200-300 $\mu\text{mol photons m}^{-2} \text{ s}^{-1}$
408 illumination for 10-25 min), allowing cells to consume internal C_i stores. When net oxygen
409 evolution ceased, aliquots of NaHCO_3 were added to the cells at 30 s intervals and the rate
410 of oxygen evolution was recorded every second using a PicoLog 1216 data logger (Pico
411 Technologies, St Neots, UK). Cumulative concentrations of NaHCO_3 after each addition
412 were as follows: 2.5, 5, 10, 25, 50, 100, 250, 500, 1000 and 2000 μM . Some of the RNA and
413 protein extraction and quantitation methods were conducted after 25 min illumination in the
414 electrode chamber to mimic a standard light pre-treatment plus C_i addition protocol.

415 **Chlorophyll extraction:** Chlorophyll was extracted from cells for normalisation of oxygen
416 evolution measurements and loading of proteins for SDS-PAGE and immunoblots.
417 Chlorophyll was extracted in 90% acetone (10 min at 60 °C) and the absorbance of the
418 supernatant was measured at 647 and 664 nm. Chlorophyll concentration was calculated
419 using the equations of Jeffrey and Humphrey (1975).

420 **Analysis of gene expression by qRT-PCR:** Quantitative reverse transcriptase PCR (qRT-
421 PCR) was used to determine the relative abundance of CCM gene transcripts. Total RNA
422 was extracted from 1×10^7 cells using TRIzol Reagent (Life Technologies, Carlsbad, CA,
423 USA). cDNA was synthesised from 500 ng total RNA using SuperScript II reverse
424 transcriptase (Life Technologies), RNaseOUT (Life Technologies) and oligo(dT)₁₈ primers
425 (Thermo Scientific, Waltham, MA, USA). Relative gene expression was determined using a
426 Rotor-Gene Q Real-Time PCR Cycler (Qiagen, Hilden, Germany). Reactions (10 μ l) used
427 SYBR Green JumpStart Taq ReadyMix (Sigma-Aldrich, St Louis, MO, USA) and gene
428 expression was calculated relative to the first time point and the reference gene *GBLP*
429 (*CBLP/RACK1*; Schloss, 1990) according to the $2^{-\Delta\Delta C_t}$ method (Livak and Schmittgen, 2001).
430 Primers were designed using the web-based tools Primer3 (*CCP1*, *CCP2*, *GBLP*, *LCIA*,
431 *LCIB*, *LCIC*, *rbcL*, *RBCS*; Rozen and Skaletsky, 2000) or QuantPrime (*CAH1*, *HLA3*, *LCI1*,
432 *LCR1*; Arvidsson et al., 2008). Primer sequences are listed in Supplemental Table S5.

433 **Detection of CCM proteins using immunoblots:** Cells (2.5×10^7) were harvested by
434 centrifugation, resuspended in 500 μ l protein extraction buffer (50 mM Bicine pH 8.0, 10 mM
435 NaHCO₃, 10 mM MgCl₂, and 1 mM dithiothreitol) and sonicated in 15 mL tubes for 15 min at
436 4 °C on high power using a Diagenode bioruptor (Diagenode, Liège, Belgium). Optimal lysis
437 conditions were previously determined by visually inspecting samples under a light
438 microscope. Unbroken cells were pelleted by centrifugation at 4,400 x *g* for 10 min at 4 °C
439 and protein levels in the supernatant (soluble protein fraction) were quantified using Bradford
440 reagent (Sigma-Aldrich). Proteins were separated on a 12% polyacrylamide gel using SDS-
441 PAGE. Sample loading was normalised by chlorophyll amount (extraction described above)
442 for both dark/light and CO₂ time courses (1.5 μ g per lane). Samples were also normalised by
443 protein (5 μ g per lane) and probed using all antibodies, which gave similar results to
444 normalisation by chlorophyll, as summarised in Supplemental Fig. S1.

445 For immunodetection, proteins were transferred electrophoretically to a PVDF membrane
446 (Bio-Rad, Hercules, CA, USA). Membranes were probed with primary antibodies raised
447 against Rubisco (*RBCS* and *rbcL*), *LCIB*, *LCIC* or *CAH1* and donkey secondary antibodies
448 (ECL anti-rabbit IgG, horse radish peroxidase-linked whole antibody, GE Healthcare,
449 Amersham, UK). Membranes were stripped using Restore Plus Western Blot Stripping
450 Buffer (Thermo Scientific) and reprobed to allow the detection of multiple proteins on a single
451 membrane.

452 **Transmission electron microscopy and immunogold localisation:** Synchronised
453 *Chlamydomonas* cells were grown to mid-log phase in 12 h:12 h dark/light cycles as
454 described above. Prior to dawn, cells were fixed and harvested either in the dark (-2D and -

455 1D) or after a light pre-treatment (-2L and -1L) in the oxygen electrode chamber. A final
456 sample was also prepared from cells harvested two hours into the light period.

457 For fixation of cells for electron microscopy, glutaraldehyde (electron microscopy grade) was
458 added to a final concentration of 0.5% (v/v) to cultures prior to harvest by centrifugation.
459 Cells were then resuspended in 0.5% (v/v) glutaraldehyde and 1% (v/v) H₂O₂ in Tris-minimal
460 medium and fixed for 30 min to 2 h at 4°C. All subsequent steps were carried out at room
461 temperature (c. 20°C).

462 Samples were postfixed and osmicated for 1 h in 1% (v/v) OsO₄, 1.5% (w/v) K₃[Fe(CN)₆]
463 and 2 mM CaCl₂. After osmication, samples were stained in 2% (w/v) uranyl acetate for 1 h
464 and serially dehydrated for 5 min each in 75, 95, and 100% ethanol followed by two
465 incubations in 100% acetonitrile. Samples were embedded in epoxy resin containing 34%
466 Quetol 651, 44% nonenyl succinic anhydride, 20% methyl-5-norbornene-2,3-dicarboxylic
467 anhydride and 2% catalyst dimethyl-benzylamine (Agar Scientific, Stansted, UK) and the
468 resin was refreshed four times over two days. Samples were degassed and cured at 60°C
469 for at least 3 h. Sections (50 nm) were obtained with a Leica Ultracut UCT Ultramicrotome
470 (Leica Microsystems) and mounted on bare 300 mesh nickel grids.

471 For immunogold labelling of Rubisco and CAH3, fixed and embedded samples were treated
472 to remove superficial osmium and unmask epitopes (Skepper, 2000). Grids were incubated
473 face down on droplets of 4% metaperiodate for 15 min and then washed with dH₂O.
474 Samples were then incubated in 1% periodic acid for 5 min and washed in dH₂O. Non-
475 specific binding sites were blocked by incubating grids in TBS-TT (Tris buffered saline with
476 0.001% Triton X-100 and 0.001% Tween20) containing 0.1% BSA (bovine serum albumin)
477 for 5 min. Primary antibodies were diluted in TBS-TT plus 0.1% BSA and incubated in humid
478 chambers for 16 h. Grids were then washed in TBS-TT and dH₂O. Grids were incubated for
479 1 h with secondary antibodies (Goat anti-rabbit 15 nm gold conjugates, BBI Solutions,
480 Cardiff, UK) diluted 1:200 in TBS-TT plus 0.1% BSA, washed with TBS-TT and dH₂O and
481 dried. The CAH3 antibody was from Agrisera AB (Vännäs, Sweden).

482 Samples were examined with a Technai G² transmission electron microscope at 120 kV (FEI
483 Company, Hillsboro, OR, USA) and imaged with AMT Image Capture Engine software
484 (Advanced Microscopy Techniques, Woburn, MA, USA). Image analysis (area
485 measurements and particle counts) was performed using ImageJ (Abramoff et al., 2004).
486 The fraction of gold particles in the pyrenoid was calculated for cells in which the pyrenoid
487 and much of the chloroplast was visible. For each cell, the number of gold particles in the
488 pyrenoid (density multiplied by area) was expressed as a percentage of the total number of
489 particles in the chloroplast (stroma plus pyrenoid). Nonspecific labelling was determined by

490 calculating the density of labelling in the cytosol and this value was deducted from both the
491 pyrenoidal and stromal densities.

492 **Acknowledgements:** Asst Prof Takashi Yamano (University of Kyoto) and Prof Martin
493 Spalding (Iowa State University) for the generous gift of antibodies (LCIB/LCIC and CAH1,
494 respectively). Dr Jeremy Skepper (Cambridge Advanced Imaging Centre) for help with
495 electron microscopy and immunogold labelling. Prof Robert Spreitzer (University of
496 Nebraska, Lincoln) for the gift of wild-type *Chlamydomonas* strain 2137 mt+. Prof John Gray
497 (University of Cambridge) for the gift of the Rubisco antibodies as well as financial support.

498 LITERATURE CITED

- 499 **Abramoff MD, Magalhaes PJ, Ram SJ** (2004) Image processing with ImageJ. *Biophot Int*
500 **11:** 36-42
- 501 **Arvidsson S, Kwasniewski M, Riano-Pachon DM, Mueller-Roeber B** (2008) QuantPrime
502 - a flexible tool for reliable high-throughput primer design for quantitative PCR. *BMC*
503 *Bioinformatics* **9:** 465
- 504 **Badger MR, Kaplan A, Berry JA** (1980) Internal inorganic carbon pool of *Chlamydomonas*
505 *reinhardtii*: evidence for a carbon dioxide-concentrating mechanism. *Plant Physiol*
506 **66:** 407-413
- 507 **Blanco-Rivero A, Shutova T, Roman MJ, Villarejo A, Martinez F** (2012) Phosphorylation
508 controls the localization and activation of the luminal carbonic anhydrase in
509 *Chlamydomonas reinhardtii*. *PLOS ONE* **7:** e49063
- 510 **Borkhsenius ON, Mason CB, Moroney JV** (1998) The intracellular localization of
511 ribulose-1,5-bisphosphate carboxylase/oxygenase in *Chlamydomonas reinhardtii*.
512 *Plant Physiol* **116:** 1585-1591
- 513 **Bozzo GG, Colman B** (2000) The induction of inorganic carbon transport and external
514 carbonic anhydrase in *Chlamydomonas reinhardtii* is regulated by external CO₂
515 concentration. *Plant Cell Environ* **23:** 1137-1144
- 516 **Brueggeman AJ, Gangadharaiah DS, Cserhati MF, Casero D, Weeks DP, Ladunga I**
517 (2012) Activation of the carbon concentrating mechanism by CO₂ deprivation
518 coincides with massive transcriptional restructuring in *Chlamydomonas reinhardtii*.
519 *Plant Cell* **24:** 1860-1875
- 520 **Colombo SL, Pollock SV, Eger KA, Godfrey AC, Adams JE, Mason CB, Moroney JV**
521 (2002) Use of the bleomycin resistance gene to generate tagged insertional mutants
522 of *Chlamydomonas reinhardtii* that require elevated CO₂ for optimal growth.
523 *Functional Plant Biology* **29:** 231-241

524 **Dionisio-Sese ML, Fukuzawa H, Miyachi S** (1990) Light-induced carbonic anhydrase
525 expression in *Chlamydomonas reinhardtii*. *Plant Physiology* **94**: 1103-1110

526 **Duanmu D, Miller AR, Horken KM, Weeks DP, Spalding MH** (2009) Knockdown of
527 limiting-CO₂-induced gene *HLA3* decreases HCO₃⁻ transport and photosynthetic Ci
528 affinity in *Chlamydomonas reinhardtii*. *Proc Natl Acad Sci USA* **106**: 5990-5995

529 **Eriksson M, Villand P, Gardestrom P, Samuelsson G** (1998) Induction and regulation of
530 expression of a low-CO₂-induced mitochondrial carbonic anhydrase in
531 *Chlamydomonas reinhardtii*. *Plant Physiol* **116**: 637-641

532 **Fang W, Si Y, Douglass S, Casero D, Merchant SS, Pellegrini M, Ladunga I, Liu P,**
533 **Spalding MH** (2012) Transcriptome-wide changes in *Chlamydomonas reinhardtii*
534 gene expression regulated by carbon dioxide and the CO₂-concentrating mechanism
535 regulator CIA5/CCM1. *Plant Cell* **24**: 1876-1893

536 **Fujiwara S, Ishida N, Tsuzuki M** (1996) Circadian expression of the carbonic anhydrase
537 gene, *Cah1*, in *Chlamydomonas reinhardtii*. *Plant Mol Biol* **32**: 745-749

538 **Giordano M, Beardall J, Raven JA** (2005) CO₂ concentrating mechanisms in algae:
539 mechanisms, environmental modulation, and evolution. *Annu Rev Plant Biol* **56**: 99-
540 131

541 **Im CS, Grossman AR** (2002) Identification and regulation of high light-induced genes in
542 *Chlamydomonas reinhardtii*. *Plant J* **30**: 301-313

543 **Jeffrey SW, Humphrey GF** (1975) New spectrophotometric equations for determining
544 chlorophylls *a*, *b*, *c*₁, and *c*₂ in higher plants, algae and natural phytoplankton.
545 *Biochem Physiol Pflanz* **165**: 191-194

546 **Karlsson J, Clarke AK, Chen ZY, Huggins SY, Park YI, Husic HD, Moroney JV,**
547 **Samuelsson G** (1998) A novel α-type carbonic anhydrase associated with the
548 thylakoid membrane in *Chlamydomonas reinhardtii* is required for growth at ambient
549 CO₂. *EMBO J* **17**: 1208-1216

550 **Kropat J, Hong-Hermesdorf A, Casero D, Ent P, Castruita M, Pellegrini M, Merchant**
551 **SS, Malasarn D** (2011) A revised mineral nutrient supplement increases biomass
552 and growth rate in *Chlamydomonas reinhardtii*. *Plant J* **66**: 770-780

553 **Livak KJ, Schmittgen TD** (2001) Analysis of relative gene expression data using real-time
554 quantitative PCR and the 2^{-ΔΔC_T} method. *Methods* **25**: 402-408

555 **Ma Y, Pollock SV, Xiao Y, Cunnusamy K, Moroney JV** (2011) Identification of a novel
556 gene, *CIA6*, required for normal pyrenoid formation in *Chlamydomonas reinhardtii*.
557 *Plant Physiol* **156**: 884-896

558 **Manuel LJ, Moroney JV** (1988) Inorganic carbon accumulation by *Chlamydomonas*
559 *reinhartii*: new proteins are made during adaptation to low CO₂. *Plant Physiol* **88**:
560 491-496

561 **Marcus Y, Schuster G, Michaels A, Kaplan A** (1986) Adaptation to CO₂ levels and
562 changes in the phosphorylation of thylakoid proteins during the cell cycle of
563 *Chlamydomonas reinhardtii*. *Plant Physiol* **80**: 604-607

564 **Meyer MT, Genkov T, Skepper JN, Jouhet J, Mitchell MC, Spreitzer RJ, Griffiths H**
565 (2012) Rubisco small-subunit α -helices control pyrenoid formation in
566 *Chlamydomonas*. *Proc Natl Acad Sci USA* **109**: 19474-19479

567 **Miura K, Yamano T, Yoshioka S, Kohinata T, Inoue Y, Taniguchi F, Asamizu E,**
568 **Nakamura Y, Tabata S, Yamato KT, Ohyama K, Fukuzawa H** (2004) Expression
569 profiling-based identification of CO₂-responsive genes regulated by CCM1 controlling
570 a carbon-concentrating mechanism in *Chlamydomonas reinhardtii*. *Plant Physiol* **135**:
571 1595-1607

572 **Moroney JV, Ma Y, Frey WD, Fusilier KA, Pham TT, Simms TA, Dimario RJ, Yang J,**
573 **Mukherjee B** (2011) The carbonic anhydrase isoforms of *Chlamydomonas*
574 *reinhardtii*: intracellular location, expression, and physiological roles. *Photosynth Res*
575 **109**: 133-149

576 **Moroney JV, Ynalvez RA** (2007) Proposed carbon dioxide concentrating mechanism in
577 *Chlamydomonas reinhardtii*. *Eukaryot Cell* **6**: 1251-1259

578 **Ohnishi N, Mukherjee B, Tsujikawa T, Yanase M, Nakano H, Moroney JV, Fukuzawa H**
579 (2010) Expression of a low CO₂-inducible protein, LCI1, increases inorganic carbon
580 uptake in the green alga *Chlamydomonas reinhardtii*. *Plant Cell* **22**: 3105-3117

581 **Price GD, Badger MR, Woodger FJ, Long BM** (2008) Advances in understanding the
582 cyanobacterial CO₂-concentrating-mechanism (CCM): functional components, Ci
583 transporters, diversity, genetic regulation and prospects for engineering into plants. *J*
584 *Exp Bot* **59**: 1441-1461

585 **Rawat M, Moroney JV** (1995) The regulation of carbonic anhydrase and ribulose-1,5-
586 bisphosphate carboxylase oxygenase activase by light and CO₂ in *Chlamydomonas*
587 *reinhardtii*. *Plant Physiol* **109**: 937-944

588 **Rozen S, Skaletsky H** (2000) Primer3 on the WWW for general users and for biologist
589 programmers. *Methods Mol Biol* **132**: 365-386

590 **Schloss JA** (1990) A *Chlamydomonas* gene encodes a G protein β subunit-like polypeptide.
591 *Mol Gen Genet* **221**: 443-452

592 **Skepper JN** (2000) Immunocytochemical strategies for electron microscopy: choice or
593 compromise. *J Microsc* **199**: 1-36

594 **Spalding MH** (2008) Microalgal carbon-dioxide-concentrating mechanisms:
595 *Chlamydomonas* inorganic carbon transporters. *J Exp Bot* **59**: 1463-1473

596 **Spalding MH, Critchley C, Govindjee, Orgren WL** (1984) Influence of carbon dioxide
597 concentration during growth on fluorescence induction characteristics of the green
598 alga *Chlamydomonas reinhardtii*. *Photosynth Res* **5**: 169-176

599 **Spalding MH, Ogren WL** (1982) Photosynthesis is required for induction of the CO₂-
600 concentrating system in *Chlamydomonas reinhardtii*. *FEBS Lett* **145**: 41-44

601 **Spalding MH, Spreitzer RJ, Ogren WL** (1983) Reduced inorganic carbon transport in a
602 CO₂-requiring mutant of *Chlamydomonas reinhardtii*. *Plant Physiol* **73**: 273-276

603 **Spreitzer RJ, Mets L** (1981) Photosynthesis-deficient mutants of *Chlamydomonas reinhardtii*
604 with associated light-sensitive phenotypes. *Plant Physiol* **67**: 565-569

605 **Spreitzer RJ, Salvucci ME** (2002) Rubisco: structure, regulatory interactions, and
606 possibilities for a better enzyme. *Annu Rev Plant Biol* **53**: 449-475

607 **Thyssen C, Hermes M, Sultemeyer D** (2003) Isolation and characterisation of
608 *Chlamydomonas reinhardtii* mutants with an impaired CO₂-concentrating mechanism.
609 *Planta* **217**: 102-112

610 **Tirumani S, Kokkanti M, Chaudhari V, Shukla M, Rao BJ** (2014) Regulation of CCM
611 genes in *Chlamydomonas reinhardtii* during conditions of light-dark cycles in
612 synchronous cultures. *Plant Mol Biol* **85**: 277-286

613 **Turkina MV, Blanco-Rivero A, Vainonen JP, Vener AV, Villarejo A** (2006) CO₂ limitation
614 induces specific redox-dependent protein phosphorylation in *Chlamydomonas*
615 *reinhardtii*. *Proteomics* **6**: 2693-2704

616 **Van K, Spalding MH** (1999) Periplasmic carbonic anhydrase structural gene (*Cah1*) mutant
617 in *Chlamydomonas reinhardtii*. *Plant Physiol* **120**: 757-764

618 **Wang YJ, Duanmu DQ, Spalding MH** (2011) Carbon dioxide concentrating mechanism in
619 *Chlamydomonas reinhardtii*: inorganic carbon transport and CO₂ recapture.
620 *Photosynth Res* **109**: 115-122

621 **Wang Y, Spalding MH** (2013) LCIB in the *Chlamydomonas* CO₂-concentrating mechanism.
622 *Photosynth Res* **121**: 185-192

623 **Yamano T, Miura K, Fukuzawa H** (2008) Expression analysis of genes associated with the
624 induction of the carbon-concentrating mechanism in *Chlamydomonas reinhardtii*.
625 *Plant Physiol* **147**: 340-354

626 **Yamano T, Tsujikawa T, Hatano K, Ozawa S, Takahashi Y, Fukuzawa H** (2010) Light and
627 low-CO₂-dependent LCIB-LCIC complex localization in the chloroplast supports the
628 carbon-concentrating mechanism in *Chlamydomonas reinhardtii*. *Plant Cell Physiol*
629 **51**: 1453-1468

630 **Yoshioka S, Taniguchi F, Miura K, Inoue T, Yamano T, Fukuzawa H** (2004) The novel
631 Myb transcription factor LCR1 regulates the CO₂-responsive gene *Cah1*, encoding a

632 periplasmic carbonic anhydrase in *Chlamydomonas reinhardtii*. Plant Cell **16**: 1466-
633 1477

634 **Figure Legends**

635 **Figure 1.** Whole cell affinity for Ci ($K_{0.5}$) measured in wild-type *Chlamydomonas* during CCM
636 induction in (A) synchronised cells during the dark to light transition and (B) in response to
637 low CO_2 in asynchronous cultures. Synchronised cells were grown in 12 h:12 h dark/light
638 cycles under low CO_2 and harvested during the third dark to light transition after dilution
639 (dawn = 0 h). Asynchronous cells were grown to mid-log phase in high CO_2 and harvested
640 following the switch to low CO_2 (t = 0 h). Values are mean \pm 1 s.e. of three to five
641 independent experiments.

642 **Figure 2.** Expression profiles of CCM genes in synchronised cells during the dark to light
643 transition. mRNA abundance was determined using qRT-PCR and normalised to mRNA
644 levels in -2D cells and to *GBLP* (control gene) expression. Growth and harvest conditions
645 were as described in Fig. 1. During the dark period (-2 and -1 h), mRNA was harvested from
646 cells taken either straight from the dark (D) or after a brief illumination in the oxygen
647 electrode chamber (L) to mimic the light pre-treatment necessary for $K_{0.5}$ measurements.
648 Values are mean \pm 1 s.e. of three to seven separate flasks harvested across at least three
649 independent experiments.

650 **Figure 3.** Expression profiles of CCM genes in asynchronous cells adapting to low CO_2 .
651 mRNA abundance was determined using qRT-PCR and normalised to mRNA levels in high
652 CO_2 -adapted cells and to *GBLP* (control gene) expression. Values are mean \pm 1 s.e. of three
653 separate flasks harvested during a single experiment.

654 **Figure 4.** Expression profiles of CCM-related proteins in synchronised cells during the dark
655 to light transition. Soluble protein extracts were separated using SDS-PAGE and used for
656 immunoblot analyses with antibodies raised against CAH1, LCIB, LCIC and Rubisco (rbcL
657 and RBCS). Sample loading was normalised by chlorophyll content. During the dark period
658 (-2 and -1 h), protein was harvested from cells taken either straight from the dark (D) or after
659 a brief illumination in the oxygen electrode chamber (L) to mimic the light pre-treatment
660 necessary for $K_{0.5}$ measurements.

661 **Figure 5.** Expression profiles of CCM-related proteins in asynchronous cells adapting to low
662 CO_2 . Soluble protein extracts were separated using SDS-PAGE and used for immunoblot
663 analyses with antibodies raised against CAH1, LCIB, LCIC and Rubisco (rbcL and RBCS).
664 Sample loading was normalised by chlorophyll content.

665 **Figure 6.** Localisation of mobile CCM components in synchronised cells during the dark to
666 light transition. Immunogold localisation was used to determine the relative abundance in the
667 pyrenoid of (A) primary photosynthetic carboxylase and pyrenoid component, Rubisco, and
668 (B) thylakoid lumen-localised carbonic anhydrase, CAH3 (n=53). Cell area (C) and pyrenoid
669 area (D) were also determined (n=80). Bars represent mean \pm 1 s.e.

Figure 1.

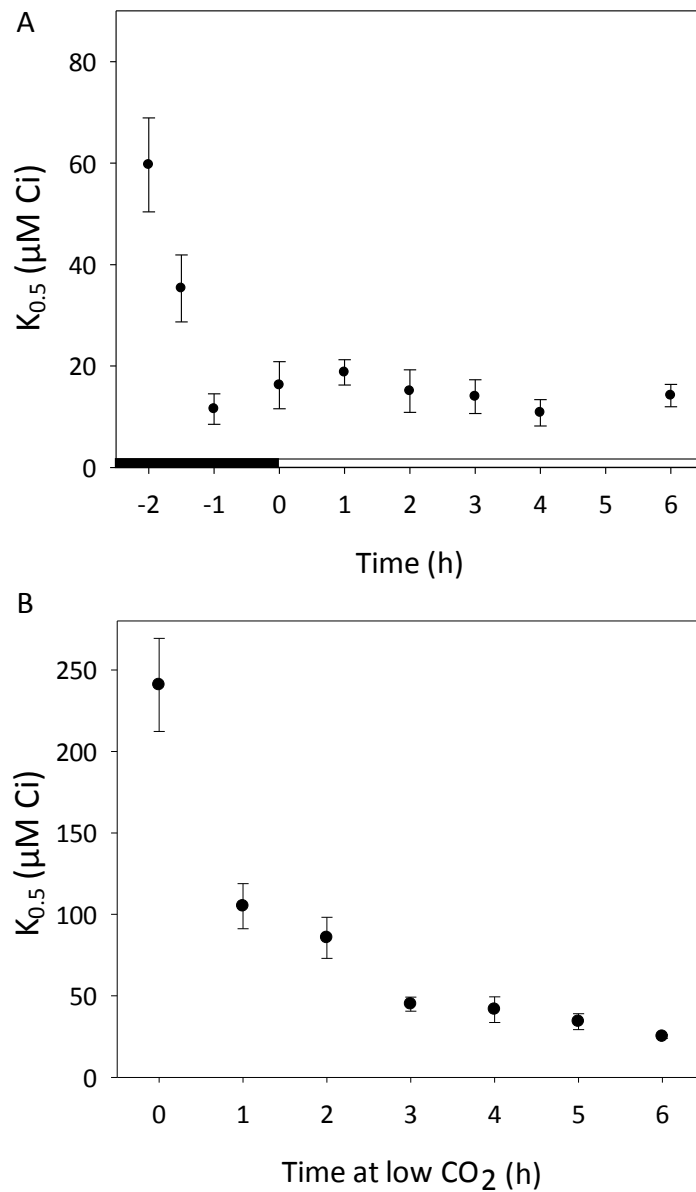


Figure 1. Whole cell affinity for CO_2 ($K_{0.5}$) measured in wild-type *Chlamydomonas* during CCM induction in (A) synchronised cells during the dark to light transition and (B) in response to low CO_2 in asynchronous cultures. Synchronised cells were grown in 12 h:12 h dark/light cycles under low CO_2 and harvested during the third dark to light transition after dilution (dawn = 0 h). Asynchronous cells were grown to mid-log phase in high CO_2 and harvested following the switch to low CO_2 ($t = 0$ h). Values are mean ± 1 s.e. of three to five independent experiments.

Figure 2.

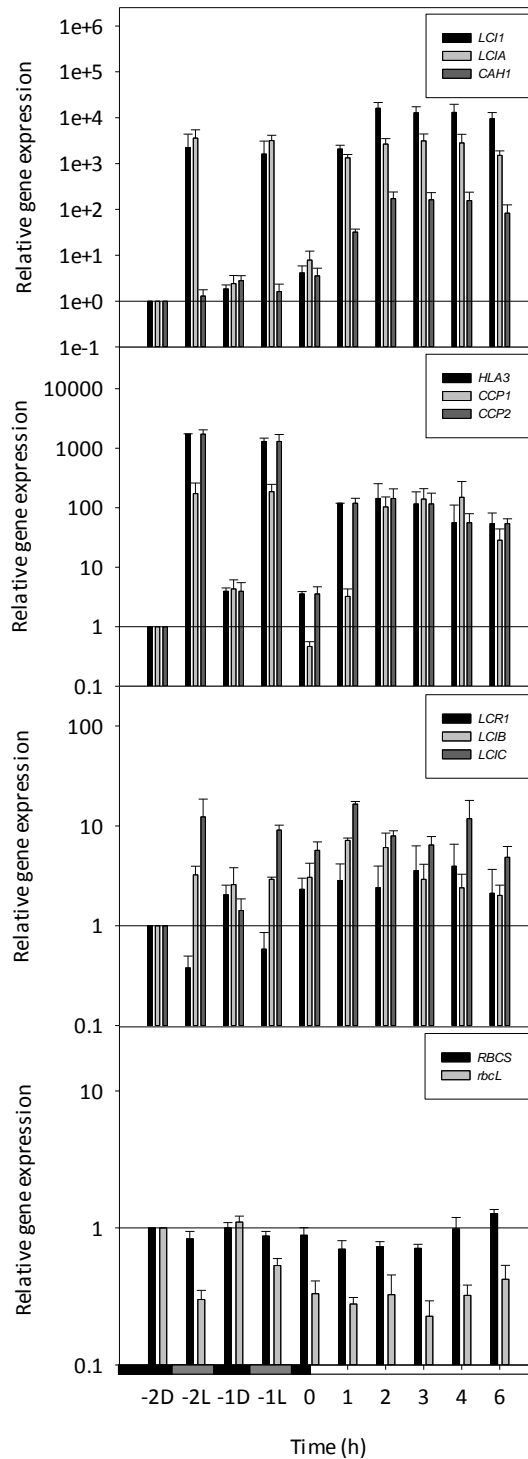


Figure 2. Expression profiles of CCM genes in synchronised cells during the dark to light transition. mRNA abundance was determined using qRT-PCR and normalised to mRNA levels in -2D cells and to *GBLP* (control gene) expression. Growth and harvest conditions were as described in Figure 1. During the dark period (-2 and -1 h), mRNA was harvested from cells taken either straight from the dark (D) or after 25 min illumination in the oxygen electrode chamber (L to mimic the light pre-treatment necessary for $K_{0.5}$ measurements). Values are mean \pm 1 s.e. of three to seven separate flasks harvested across at least three independent experiments.

Figure 3.

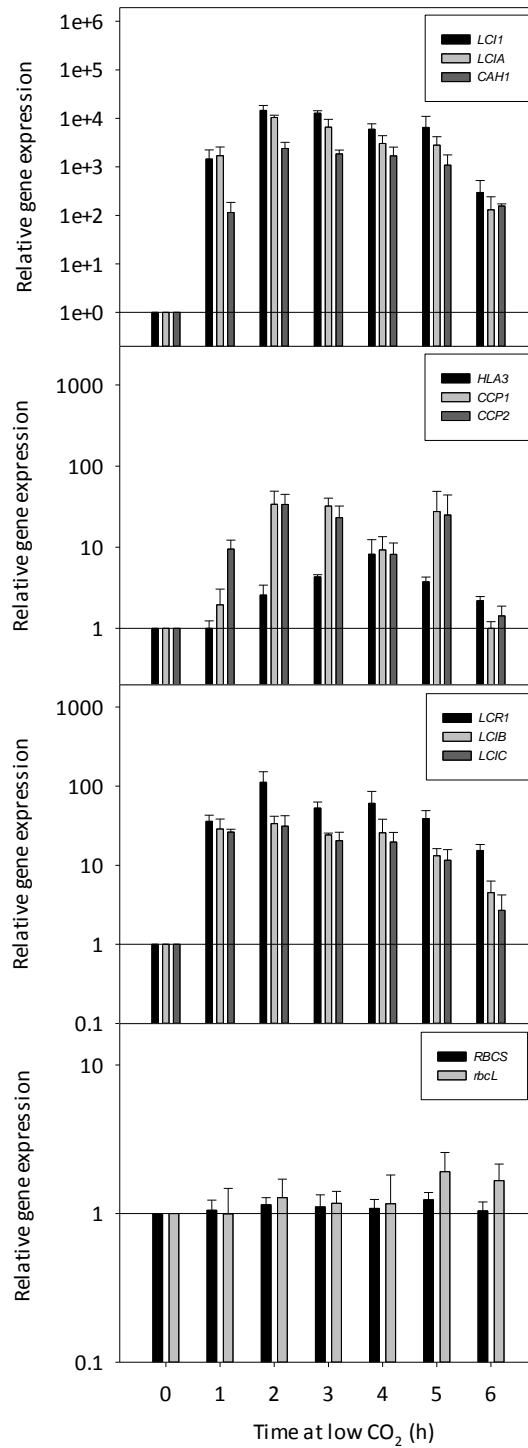


Figure 3. Expression profiles of CCM genes in asynchronous cells adapting to low CO₂. mRNA abundance was determined using qRT-PCR and normalised to mRNA levels in high CO₂-adapted cells and to *GBLP* (control gene) expression. Values are mean \pm 1 s.e. of three separate flasks harvested during a single experiment.

Figure 4.

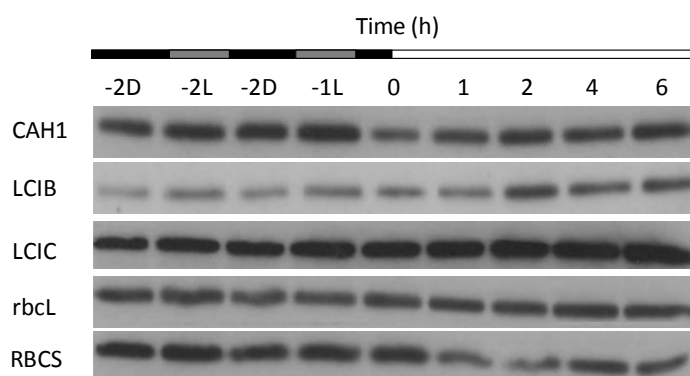


Figure 4. Expression profiles of CCM-related proteins in synchronised cells during the dark to light transition. Soluble protein extracts were separated using SDS-PAGE and used for immunoblot analyses with antibodies raised against CAH1, LCIB, LCIC and Rubisco (rbcL and RBCS). Sample loading was normalised by chlorophyll content. During the dark period (-2 and -1 h), protein was harvested from cells taken either straight from the dark (D) or after 25 min illumination in the oxygen electrode chamber (L) to mimic the light pre-treatment necessary for $K_{0.5}$ measurements.

673

Figure 5.

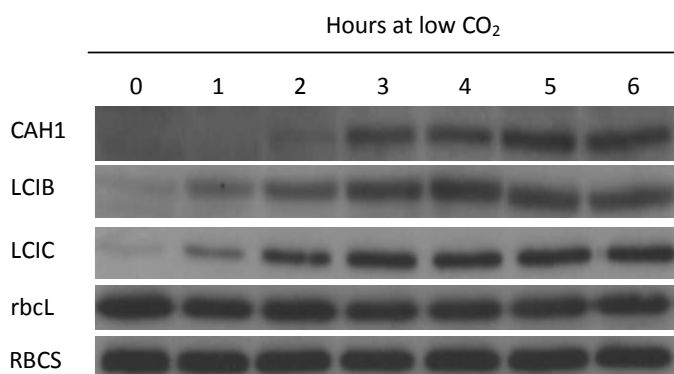


Figure 5. Expression profiles of CCM-related proteins in asynchronous cells adapting to low CO₂. Soluble protein extracts were separated using SDS-PAGE and used for immunoblot analyses with antibodies raised against CAH1, LCIB, LCIC and Rubisco (rbcL and RBCS). Sample loading was normalised by chlorophyll content.

674

Figure 6.

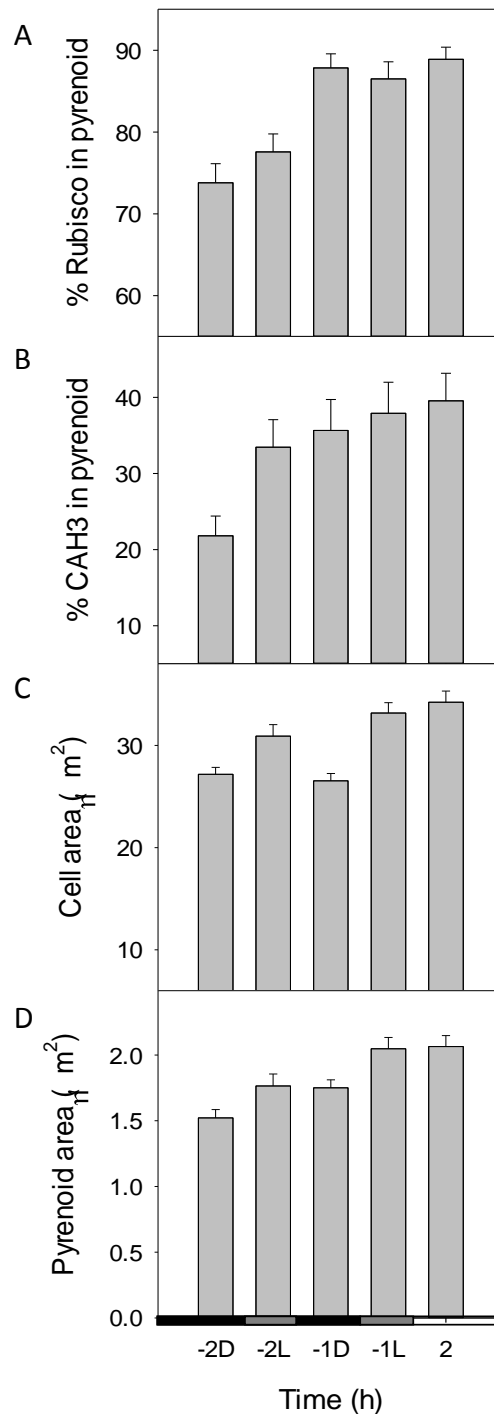


Figure 6. Localisation of mobile CCM components in synchronised cells during the dark to light transition. Immunogold localisation was used to determine the relative abundance in the pyrenoid of (A) primary photosynthetic carboxylase and pyrenoid component, Rubisco, and (B) thylakoid lumen-localised carbonic anhydrase, CAH3 (n=53). Cell area (C) and pyrenoid area (D) were also determined (n=80). Bars represent mean ± 1 s.e.

676 **Supplemental Material**

677 **Supplemental Table S1.** Relative mRNA levels of CCM genes at the first time point of
 678 dark/light (-2D) and CO₂ response (0 h) time course experiments. Mean ΔCt (Ct_(CCM gene) –
 679 Ct_(GBLP)) values of three biological replicates are shown with one standard error of the mean
 680 (s.e.). The final column compares ΔCt values for the dark/light time course to the CO₂
 681 response. Transcripts were determined to be present in greater (>, p<0.05), lesser (<,
 682 p<0.05) or equal (=, p≥0.05) abundance in -2D cells (D/L) compared to 0 h cells (CO₂) as
 683 supported by a t-test. Note that a ten-fold increase in mRNA abundance will result in a
 684 decrease in Ct of approximately 3.3.

Gene	D/L time course, ΔCt	CO ₂ time course, ΔCt	D/L vs CO ₂ (-2D vs 0 h)
<i>CAH1</i>	7.90 ± 0.22	12.67 ± 0.66	>
<i>CCP1</i>	13.79 ± 0.80	14.00 ± 0.69	=
<i>CCP2</i>	12.32 ± 0.50	11.25 ± 0.45	=
<i>HLA3</i>	12.56 ± 0.17	8.83 ± 0.96	<
<i>LCI1</i>	10.99 ± 0.11	10.75 ± 0.31	=
<i>LCIA</i>	13.20 ± 0.51	13.66 ± 0.16	=
<i>LCIB</i>	4.24 ± 0.16	5.88 ± 0.61	=
<i>LCIC</i>	8.15 ± 0.22	8.59 ± 0.47	=
<i>LCR1</i>	6.48 ± 0.96	10.15 ± 0.52	>
<i>rbcL</i>	-5.51 ± 0.02	-3.36 ± 0.52	>
<i>RBCS</i>	-5.06 ± 0.05	-5.45 ± 0.16	<

685

686 **Supplemental Table S2.** Relative mRNA levels of CCM genes at maximum expression
687 during dark/light (excluding the pre-dawn light treatment) and CO₂ response time course
688 experiments. Mean ΔCt ($Ct_{(CCM\ gene)} - Ct_{(GBLP)}$) values of three biological replicates are shown
689 with one standard error of the mean (s.e.). The time when maximum mRNA expression
690 occurred is also shown as Max. (h). The final column compares ΔCt values for the dark/light
691 time course to the CO₂ response. Transcripts were determined to be present in greater ('>',
692 $p < 0.05$), lesser ('<', $p < 0.05$) or equal ('=', $p \geq 0.05$) abundance in D/L compared to CO₂ cells
693 as supported by a t-test.

Gene	D/L time course		CO ₂ time course		D/L vs CO ₂ (max. exp.)
	ΔCt	Max. (h)	ΔCt	Max. (h)	
<i>CAH1</i>	-3.20 ± 0.17	3	-3.12 ± 0.41	2	=
<i>CCP1</i>	0.34 ± 0.29	4	1.04 ± 0.44	2	=
<i>CCP2</i>	8.39 ± 0.27	2	6.94 ± 0.89	2	<
<i>HLA3</i>	6.64 ± 0.26	4	5.19 ± 0.36	4	<
<i>LC11</i>	5.94 ± 0.26	2	4.39 ± 0.24	2	=
<i>LCIA</i>	0.64 ± 0.34	3	0.85 ± 0.36	2	=
<i>LCIB</i>	3.45 ± 0.27	1	3.99 ± 0.32	2	=
<i>LCIC</i>	3.51 ± 0.10	1	4.52 ± 0.27	2	=
<i>LCR1</i>	1.61 ± 0.18	4	0.64 ± 0.58	2	<
<i>rbcL</i>	-5.76 ± 0.04	-1	-5.36 ± 0.17	5	>
<i>RBCS</i>	-3.80 ± 0.09	6	-5.51 ± 0.02	5	>

694

695 **Supplemental Table S3.** Relative expression of CCM genes in synchronised cells during
 696 the dark to light transition. mRNA abundance was determined using qRT-PCR and values
 697 shown are normalised to mRNA levels from the first time point (-2D) cells and to *GBLP*
 698 (control gene) expression. See also Fig. 2 and Fig. S1.

Gene	Time (h)								
	-2L	-1D	-1L	0	1	2	3	4	6
<i>CAH1</i>	1.3	2.8	1.6	3.3	26	130	160	120	64
<i>CCP1</i>	170	3.9	190	0.7	100	140	180	200	120
<i>CCP2</i>	1700	3.4	1300	2.9	90	97	92	61	48
<i>HLA3</i>	61	2.0	250	1.9	4.1	150	150	200	58
<i>LCI1</i>	2200	1.3	1600	5.9	2300	12,000	10,000	11,000	7000
<i>LCIA</i>	3600	2.1	3200	7.4	970	1800	2400	2000	1100
<i>LCIB</i>	3.2	2.0	2.9	2.4	5.3	4.4	2.4	1.8	1.4
<i>LCIC</i>	12	1.3	9.1	4.3	13	5.7	5.4	7.7	3.5
<i>LCR1</i>	0.38	2.0	0.58	2.3	2.8	2.4	3.6	4.0	2.1
<i>rbcL</i>	0.30	1.1	0.53	0.33	0.28	0.33	0.23	0.32	0.42
<i>RBCS</i>	0.83	1.0	0.87	0.89	0.70	0.73	0.71	0.98	1.3

699

700 **Supplemental Table S4.** Relative expression of CCM genes in asynchronous cells adapting
 701 to low CO₂. mRNA abundance was determined using qRT-PCR and normalised to mRNA
 702 levels in high CO₂-adapted cells (t = 0 h) and to *GBLP* (control gene) expression. Values
 703 listed under Bruegg. refer to the relative induction of CCM genes observed in wild-type
 704 Chlamydomonas cells after 180 min adapting to very low CO₂ (Brueggeman et al., 2012,
 705 Supplemental Dataset 1). See also Fig. 3 and Fig. S1.

Gene	Time at low CO ₂ (h)						Bruegg.
	1	2	3	4	5	6	
<i>CAH1</i>	120	2400	1800	1700	1100	160	670
<i>CCP1</i>	4.7	29	22	8.6	22	0.86	2000
<i>CCP2</i>	17	32	20	8.2	16	1.4	120
<i>HLA3</i>	0.93	3.4	6.0	10	5.2	3.4	40
<i>LCI1</i>	1500	15,000	13,000	5900	6500	300	3000
<i>LCIA</i>	1700	10,000	6600	3000	2800	130	4200
<i>LCIB</i>	29	34	24	26	13	4.5	26
<i>LCIC</i>	26	31	20	20	12	2.7	16
<i>LCR1</i>	36	110	53	61	39	15	53
<i>rbcL</i>	1.0	1.3	1.2	1.2	1.9	1.7	-
<i>RBCS</i>	1.1	1.1	1.1	1.1	1.2	1.0	-

706

Supplemental Table S5. List of primers used in this study.

Gene	Forward primer (5' to 3')	Reverse primer (5' to 3')
<i>CAH1</i>	TGTGCACCAGGTGACTGAGAAG	TCGCAAAGATGGGCTCAAGCAG
<i>CCP1</i>	TACTCGTCCACGATGGACTG	ATGTGCTCCACGTTCTCCTC
<i>CCP2</i>	AGTACAGCACTACCATTGAC	ATGTGCTCCACGTTCTCCTC
<i>GBLP</i>	AACACCGTGACCGTCTCC	TGCTGGTGATGTTGAACTCG
<i>HLA3</i>	AGAAGCTTAAGGACCAGGATGGC	AGTTGACGTGGGACAGCAGA
<i>LC11</i>	TCCAGTTCGAGCTGTTTGTGTTCC	AGCAGGAAGAAGATGGCGTTGATG
<i>LC1A</i>	CTCCTCCTCAAGTGTATGAGAACG	CAGAGCAAATAGCAGCTTGG
<i>LC1B</i>	GAGCTGATCAAGCACTTC	CCTCAATCTTGTCTTCA
<i>LC1C</i>	CGTCCATGGAGTTCATTGC	ATGCGCTTCTCCAGGTAGC
<i>LCR1</i>	GCGCACAGTCCCTTCGTCTAATTC	AGCGATCTCGGTCCAACCTGTTAC
<i>rbcL</i>	GGTGACCACCTTCACTCTGG	TCACCGAAGATTTCAACTAAAGC
<i>RBCS</i>	GCGTGTCTTGCCTGTACTACG	CTGCTTCTGGTTGTCTGAAGG

Supplemental Figure S1. Summary of relative changes in mRNA (solid line) and protein normalised by chlorophyll (dotted line) accompanying CCM induction in (left) synchronous cultures during the dark to light transition and (right) asynchronous cultures adapting to low CO₂. The black dashed line in the dark/light time course represents relative protein levels determined by protein-normalised SDS-PAGE and immunoblots. The vertical red dashed lines indicate the time at which CCM activity reached maximum levels as determined by oxygen evolution measurements (Fig. 1).

